

## WAVY FLOW ALONG OSCILLATING WALL

Václav SOBOLÍK and Jiří DRAHOŠ

*Institute of Chemical Process Fundamentals,  
Czechoslovak Academy of Sciences, 165 02 Prague - Suchbát*

Received November 19th, 1980

A capacitance probe for the measurement of a local liquid film thickness was developed and tested. Characteristics of wavy flows of Newtonian (glycerol) and non-Newtonian liquids (aqueous solution of carboxymethylcellulose and kaolin suspension in water) along a vertical wall were measured by the probe. Attention was also devoted to the influence of wall oscillations upon waves on the film surface. The measured data on wavy flow of glycerine and partially also on carboxymethylcellulose (flow behaviour index  $n = 0.86$ ) were in a good agreement with Kapitza theory based, besides others, on the assumption of the sine shape of waves. However the theory cannot be used even as the first approximation for description of wavy flow of kaolin suspension ( $n = 0.14$ ).

Liquid film flow occurs in a wide variety of heat and mass transfer equipments. There are different regimes of the flow in dependence on Reynolds number. Relatively high transfer rate is achieved in a wavy regime. While the wavy flow of low-consistent liquids can be easily realized by the mere gravity force, the mechanical energy necessary for intensive medium transport in high-consistent liquids must be supplied in another way, *e.g.* by a close-clearance agitators used for film evaporators<sup>1</sup>. Other possibility of intensification of transport processes is oscillatory and joint wavy motion of liquid by the oscillating wall of equipment. This way seems to be particularly advantageous for highly pseudoplastic liquids exhibiting expressive decrease of apparent viscosity by oscillations<sup>2</sup>.

Many works summarized in papers by Dukler<sup>3</sup> (theoretical approaches) and by Hewitt<sup>4</sup> (experimental methods) deal with modelling of wavy structure on the flow of Newtonian liquids. However, the problem of wavy flow of non-Newtonian liquids has been treated only recently<sup>5-8</sup>. Theoretical approaches are based on the viscosity function represented by the power law model and have an asymptotic character. All solutions hold exactly for the flow behaviour index  $n \rightarrow 1$ . Wavy flow of highly pseudoplastic liquids ( $n < 0.5$ ) represents a problem again for an order of magnitude more complex and up to this time unsolved.

Aim of this experimental work is 1) to test the applicability of a constructed probe for contactless measurement of wavy flow characteristics and 2) to study the influence of wall oscillations on the wavy flow characteristics of Newtonian and non-Newtonian liquids.

## EXPERIMENTAL

### Equipment and Procedures

Apparatus for measurement of vibration effects on liquid film thickness<sup>9</sup> was extended by the capacitance probe which renders instantaneous film thickness measurement possible. A couple of needles connected with electronical stop-watch was placed on the capacitance probe for contact measurement of wave celerity. A schematic diagram of the apparatus appears in Fig. 1. A vertical duralumin plate 1, 150 mm wide and 600 mm long, was connected to an electromagnetic vibrator 2. The vibrator with the plate was suspended on a balance which was connected to balance 3. Liquid was distributed by a slit distributor 4 to the plate and after flowing down the plate the liquid entered a collection trough 5 from which it was recirculated. The plate oscillated vertically with frequency 40 Hz and amplitude adjustable to the magnitude of 2.2 mm.

The principles of the capacitance method for film thickness measurement are following: the dry plate 1 and sensing element of the probe 6 constitute a condenser, the capacity of which depends on normal distance of surfaces of the plate and sensing element. A calibration of capacitance (or another output signal depending on capacitance) in dependence on the distance between plate and the probe can be prepared by rectangular displacement of the probe against the plate. Under the assumption, that the dielectrical constant of the liquid flowing along the plate is negligibly small as compared with the dielectrical constant of air, the point on the calibration curve corresponding to the measured capacitance can be regarded as the thickness of air gap. The liquid film thickness is then calculated from the adjusted distance of the probe from the plate and the determined air gap thickness. If the size of the sensing element of the probe is much smaller than the wave length, the local thickness as function of time can be recorded by a convenient apparatus.

A sketch of capacitance probe with schematic diagram is given in Fig. 2. A brass circular plate 1 of diameter 3 mm creates the sensing element of the probe. The circular plate is placed in a teflon envelope 2, which is shielded by a brass housing 3. The measured capacity creates one arm of an AC bridge, which is excited by an astable multivibrator A. The unbalance of the bridge is detected by a differential transducer C with direct voltage output. The direct voltage obtained is conducted by a shielded cable to an amplifier 6 with output range 0—1 V. For the compensation of temperature a diode B is placed in the probe.

During the measurements the capacitance probe was located at the 534 mm distance from the leading edge of the distributor. The distance between the probe and the dry plate was 5 mm. The output signal of the amplifier was filtered by a low-pass filter with the cutoff frequency 16 Hz and was sampled by a data acquisition unit with frequency  $f_v = 20$  Hz. The sampled data of 60 seconds long realizations were recorded on a punch tape and after recounting according to the calibration curve of the probe were further analysed.

The wave celerity was calculated from the time, which a wave needed for covering the distance (9.4 mm) between the needles of the electronical stop-watch. Practical measurement of the time interval was performed by slow approach of the needles by a micrometric screw towards the film surface until the needles contacted a crest of a wave successively.

Reproducibility of the film thickness measurement equal to about 2% was estimated on the basis of the evaluated probe sensitivity.

Check and mean thickness measurement independent of the capacitance probe was performed by weighing of the wetted plate and successive calculation from the liquid hold-up. The difference of less than 10% was obtained which can be explained by uneven liquid distribution on the plate.

## Liquids

Measurements were carried out on aqueous solution of glycerol and carboxymethylcellulose and aqueous suspension of kaolin. For reliability of the celerity measurement by electrical stop-watch controlled by the couple of needles, the electrical conductance of the glycerol had to be increased by addition of KOH.

CMC was prepared by dissolving 3.5% by weight of Lovosa (product of SCHZ, Lovosice) in tap water. The viscosity function of CMC can be very well approximated by the power law model. The viscosity function of the studied 26% weight suspension of kaolin Sedlec Ia in tap water can be also approximated by the power model in the range of dominated shear rates. Physical properties of the studied liquids are summarized in Table I.

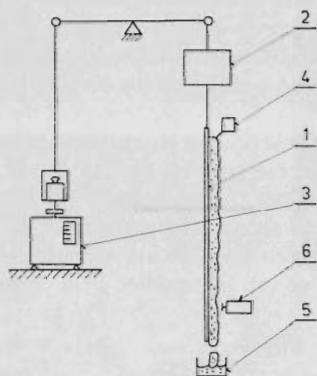


FIG. 1

Experimental apparatus. 1 Duralumin plate, 2 electromagnetical vibrator, 3 balance, 4 slit distributor, 5 collection trough, 6 capacitance probe

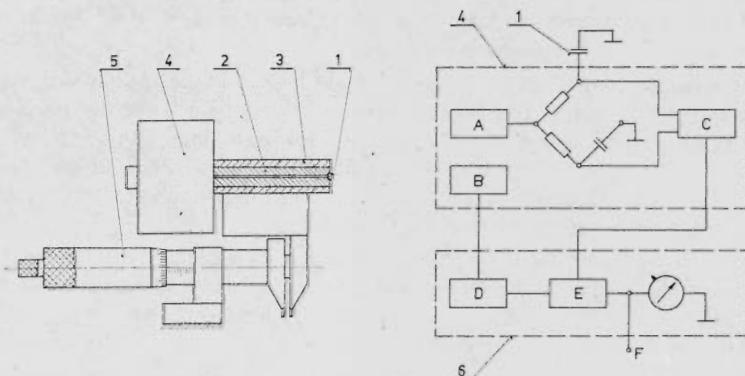


FIG. 2

Capacitance probe. *a* Section, *b* schematic diagram of capacitance probe. 1 Brass plate, 2 teflon envelope, 3 brass housing, 4 case with electronics, 5 micrometric screw, 6 amplifier, A astabil multivibrator, B diode, C differential transducer, D amplifier, E mixer + amplifier, F output

## THEORETICAL

Let us consider a liquid with viscosity function given by the power law model

$$\tau = K\dot{\gamma}^n \quad (1)$$

flowing in laminar wavy film along a vertical wall oscillating in vertical direction (Fig. 3). Under the assumption of sufficiently wide plate the flow can be considered two-dimensional, that is  $v_z = 0$ . Reynolds number, defined by the relation

$$Re = 12g^{-1}[n/(2n+1)(\rho g/K)^{1/n}]^{3n/(2n+1)} Q^{(n+2)/(2n+1)} \quad (2)$$

in which liquid flow rate and parameters of the viscosity function appeared, was chosen as one of the parameters describing the given system. Another independent parameter, amplitude of wall oscillations  $a$ , was used for description of the influence of wall oscillations on wavy flow characteristics.

Wave amplitude  $\alpha$  (further on expressed by use of film thickness  $\delta$ ), wave celerity  $c$  and wave length  $\lambda$  (Fig. 3) are the characteristics describing wave flow. Wave celerity was measured directly. For determination of other characteristics we start from a sequence  $N$  of discrete values of local film thickness ( $\delta_i$ ),  $i = 1, 2, \dots, N$ , obtained for certain values of  $Re$  and  $a$  by the procedure described in the experimental part. With respect to the algorithm of fast Fourier transform used for estimation of power spectral density, the value of  $N$  was chosen  $N = 1024$ . For the used sampling frequency  $f_v = 20$  Hz it corresponded to the record of fifty seconds long realization.

Local film thickness can be expressed by the relation<sup>10</sup>

$$\delta = \delta_0(1 + \varphi), \quad (3)$$

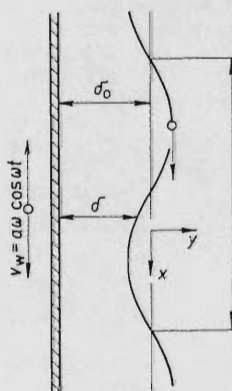


FIG. 3

Flow situation. For explanation see Theoretical

where  $\delta_0$  stands for the mean film thickness and  $\varphi(x, t)$  is a function describing the shape of film surface.

If we start in the first approximation from the sine shape of waves

$$\varphi = \alpha \sin(2\pi x/\lambda) \quad (4)$$

we can arrive by substitution of Eqs (3) and (4) into relation defining the variance of the quantity  $\delta$

$$\text{var}(\delta) = E[(\delta - E[\delta])^2] \quad (5)$$

TABLE I  
Physical parameters of liquids

Quantity	Glycerol at 25°C	CMC at 24.2°C	Kaolin at 21.3°C
Flow behaviour index $n$	1	0.86	0.14
Coefficient of consistency (Pa s <sup>n</sup> )	0.11	0.8	18
Density (kg m <sup>-3</sup> )	1 220	1 000	1 220
Surface tension (N m <sup>-1</sup> )	0.061	0.071	0.094

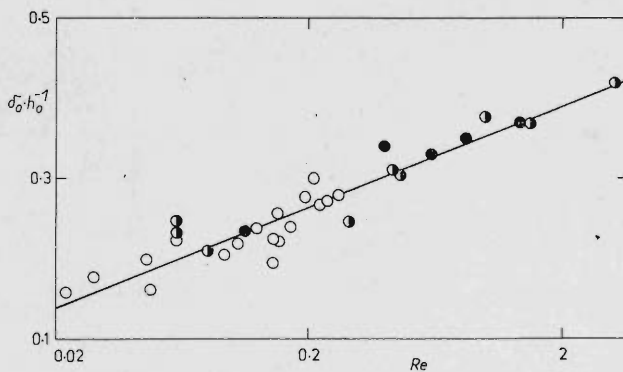


FIG. 4

Critical thickness of kaoline film. Solid line corresponds to Eq. (13),  $\bullet$   $K = 13$  Pa s<sup>n</sup>,  $\circ$   $K = 18$  Pa s<sup>n</sup>,  $\circ$   $K = 25$  Pa s<sup>n</sup>

to relation for the dimensionless amplitude of the sine wave

$$\alpha = \sqrt{(2s^2)/\delta_0}, \quad (6)$$

where the variance of  $\delta$  is substituted by its estimation

$$s^2 = 1/(N - 1) \sum_{i=1}^N (\delta_i - \delta_0)^2. \quad (7)$$

Estimation of the mean value  $\delta_0$  is given by the relation

$$\delta_0 = (1/N) \sum_{i=1}^N \delta_i. \quad (8)$$

Probability density expressing the distribution of local film thickness values can be estimated by means of histogram, which for given sequence  $(\delta_i)$ ,  $i = 1, 2, \dots, N$ , indicated the number of occurrence of sequence values pertaining to individual class intervals  $\Delta\delta$ , on which the span of values  $\delta_1, \delta_2, \dots, \delta_N$  is divided.

Wave length  $\lambda$  (Fig. 3) is given by wave celerity  $c$  and wave frequency  $f$ ,

$$\lambda = c/f. \quad (9)$$

For determination of wave frequency the spectral analysis of the sequence  $(\delta_i)$  was taken. Power spectral density was estimated for the sequence of frequencies

$$f_k = kf_v/N, \quad k = 0, 1, \dots, N - 1 \quad (10)$$

by means of the algorithm of the fast Fourier transform (FFT) from the relation<sup>11</sup>

$$G_k = 2/(f_v N) \left| \sum_{m=0}^{N-1} (\delta_m - \delta_0) \exp(-j 2\pi mk/N) \right|^2. \quad (11)$$

Wave frequencies were then determined from the shape of power spectrum *i.e.* from the dependence of the power spectral density  $G_k$  on frequency  $f_k$ .

Instead of the wave celerity, the dimensionless celerity  $z$  defined by the relation

$$z = c\delta_0/Q \quad (12)$$

is further used.

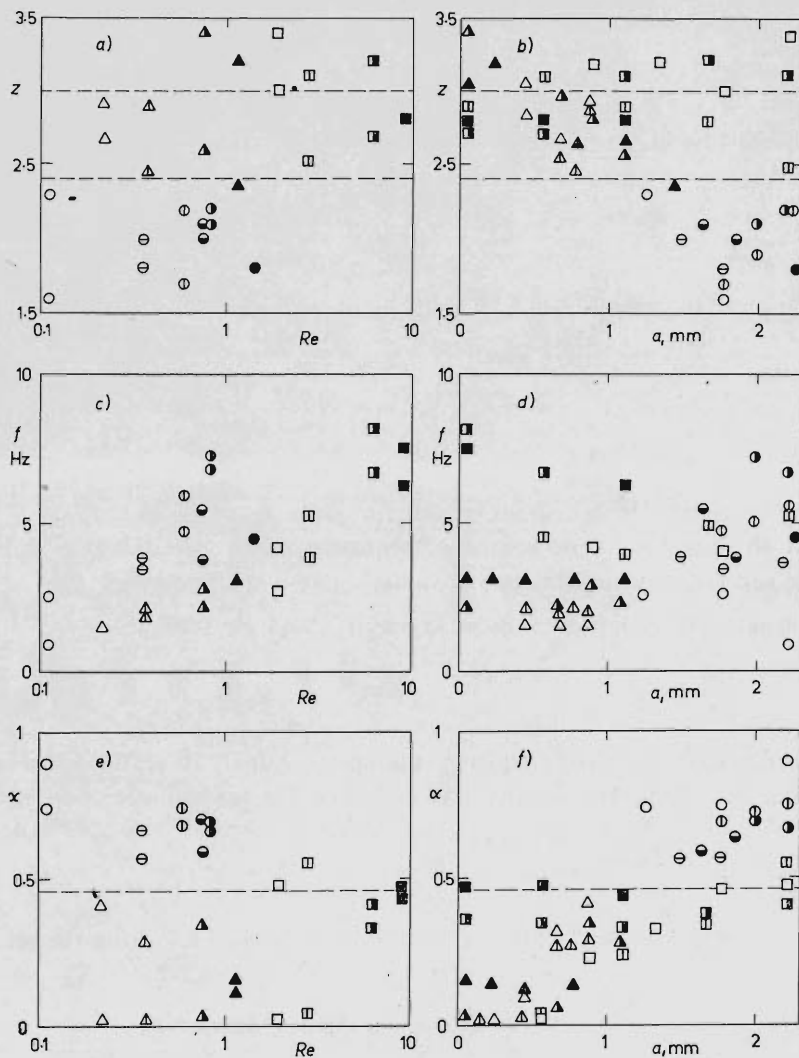


FIG. 5

Dependence of dimensionless wave celerity  $z$ , (dashed lines  $z = 3$  and  $z = 2.4$  are first and second approximations of Kapitza<sup>10</sup> respectively), wave frequency  $f$  and wave amplitude  $\alpha$  ( $\alpha = 0.44$  Kapitza's theoretical value) on Reynolds number and wall oscillations amplitude. Square points stand for glycerol, triangular points for CMC and circular points for kaolin. There are only maximum and minimum values measured at  $Re = \text{const.}$  in Figs *a, c, e*. For better orientation in Figs *b, d, f*, different values of Reynolds number are designated by different filler of points

## RESULTS AND DISCUSSION

While the wavy flow of glycerol and CMC on motionless wall was achieved by increasing the flow rate – for the glycerol at  $Re \approx 2.8$ , for CMC at  $Re \approx 1.15$  – the kaolin suspension flow on the motionless wall was laminar and nonwavy even at the highest Reynolds number achieved  $Re = 1.43$ . Wavy flow was achieved only when the suspension was “liquified” by wall oscillations. The dependence of the mean film thickness of the kaolin suspension at which wavy flow appears, normalized

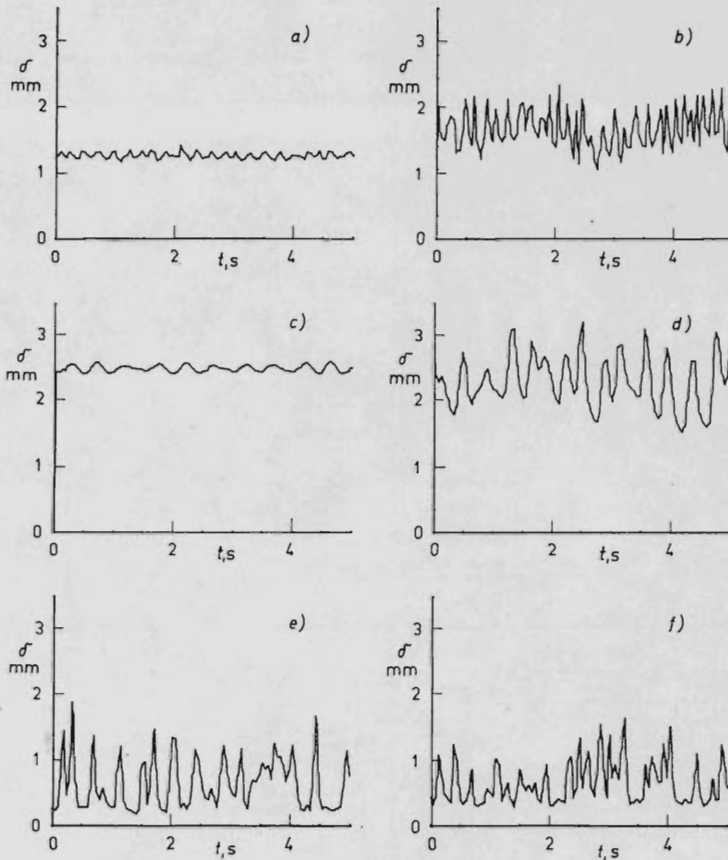


FIG. 6

Local film thickness as a function of time. Glycerol,  $Re = 2.8$ , a)  $a = 0.55$  mm, b)  $a = 2.2$  mm, CMC,  $Re = 0.76$ , c)  $a = 0$  mm, d)  $a = 1.08$  mm, kaolin,  $Re = 0.113$ , e)  $a = 1.25$  mm, f)  $a = 1.76$  mm



by the film thickness on the motionless wall, on  $Re$  is demonstrated in Fig. 4 (most data are taken from the study<sup>9</sup>). The line

$$\delta_0/h_0 = 0.35 + 0.056 \ln Re \quad (13)$$

was obtained by processing the experimental data by a least-squares procedure. The region of wavy flow lies under the line. No change of film thickness was found out at the transition of the nonwavy to the wavy flow of the glycerol (in Fig. 4 it can be represented by the line  $\delta_0 h_0^{-1} = 1$ ). The CMC solution flow has been wavy at  $Re > 1.15$  even on the motionless wall ( $\delta_0 h_0^{-1} = 1$ ); for  $Re < 1.15$ , two values of critical film thickness were determined, namely  $\delta_0 h_0^{-1} = 0.89$  and  $0.86$  at  $Re = 0.38$  and  $0.22$  respectively.

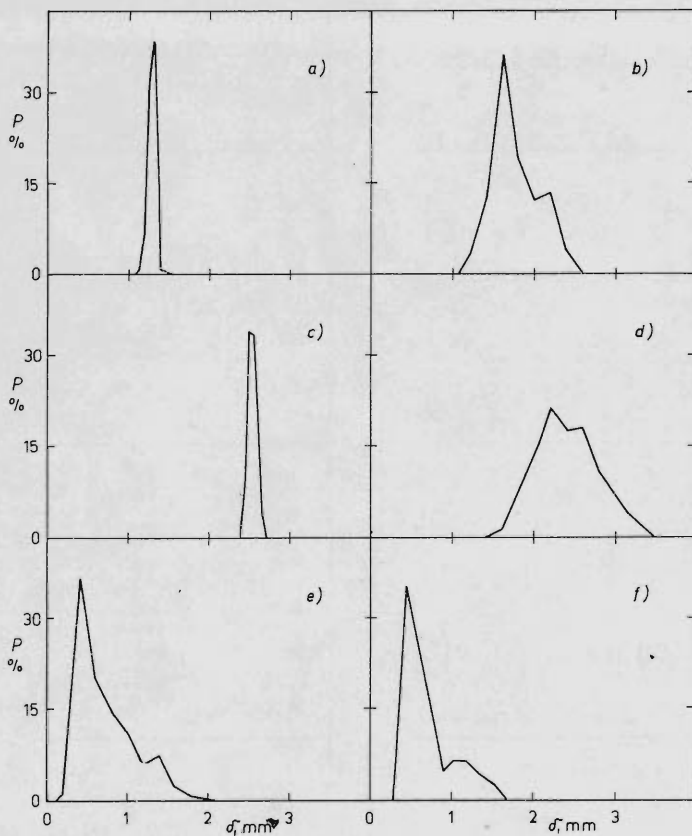


FIG. 7

Relative frequency polygons. Notation a) to f) as for Fig. 6.

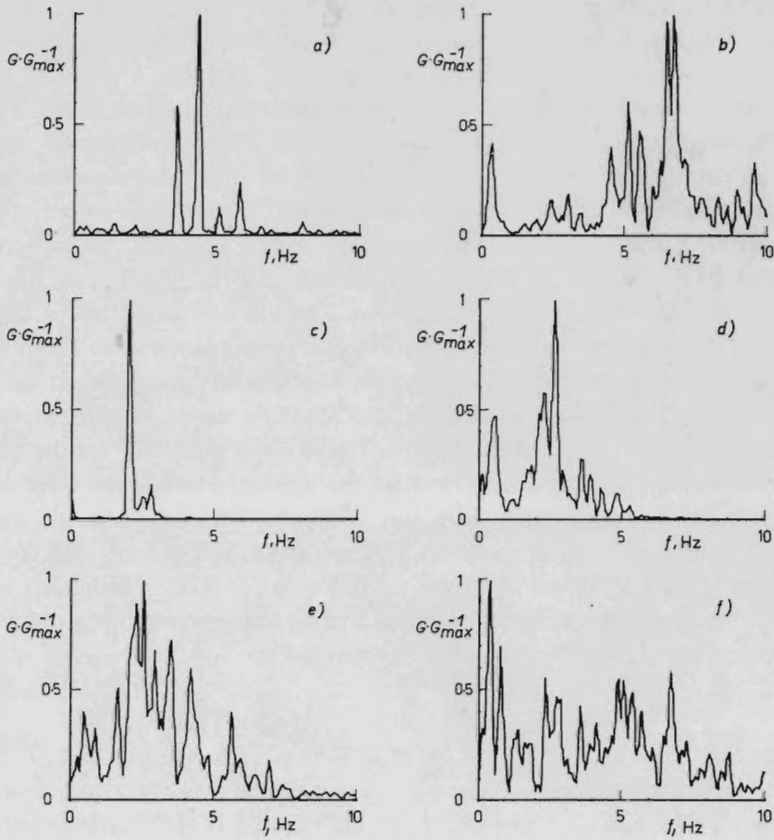


FIG. 8  
Power spectrum. Notation a) to f) as for Fig. 6

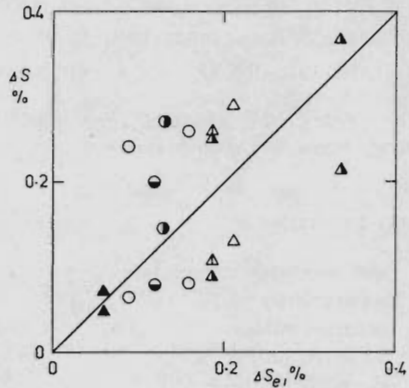


FIG. 9  
Relative enhancement of film surface. Symbols as for Fig. 5

Measured data on the dimensionless celerity  $z$ , frequency  $f$  and amplitude  $\alpha$  are summarized in Fig. 5 in dependence on Reynolds number and the wall oscillations amplitude. Representative records of the local film thickness are shown in Fig. 6, the corresponding relative frequency polygons and power spectra are in Fig. 7 and Fig. 8 respectively. Following facts were found out: a) wave celerity of any studied liquid does not depend on  $Re$ , in the case of glycerol and CMC not even on the wall oscillations amplitude. In accordance with Kapitza<sup>10</sup> theory most values of the wave celerity of the glycerol as well as CMC lie in interval (2.4; 3), that is between the second and the first Kapitza's approximations; b) wave frequency of all three liquids increases with increasing  $Re$ ; the effect of wall oscillations amplitude is represented above all by the frequency spectrum extension and consequently wave length spectrum extension; c) wave amplitude of the kaolin is practically independent on the wall oscillations amplitude; for the glycerol and CMC it holds only at higher values of  $Re$ , that is in the cases, when the flow has a wavy character on the motionless wall. Under condition of nonwavy flow on the motionless wall, the wave amplitude of glycerol and CMC increases with this quantity. Different shape of waves with kaolin (rib shape) in comparison with glycerol and CMC can be seen from Fig. 6. The difference is more remarkable from the difference of relative frequencies in Fig. 7.

Relative surface enhancement at wavy flow in comparison with nonwavy flow is often discussed. Tailby and Portalski<sup>12</sup> presented relation

$$\Delta S = (\pi\alpha\delta_0/\lambda)^2 [1 + g\alpha\lambda^3/(16\delta_0\sigma\pi^3)] \cdot 100. \quad (14)$$

For some experiments the relative surface enhancement was evaluated both from the capacitance probe records ( $\Delta S_e$ ) and from the relation (14). The results are plotted in Fig. 9; points with the lower value of  $\Delta S$  correspond to the amplitude calculated from the variance and points with the higher values of  $\Delta S$  correspond to the one half of the difference between the maximum and the minimum film thickness. The order of the surface enhancement is equal to the tenths of percent and that is why the surface enhancement cannot be responsible for as high as sixfold enhancement of transfer rate of  $\text{CO}_2$  into kaolin suspension measured on oscillating wall<sup>13</sup>.

*The authors thank Messrs O. Pavlik and J. Zima from the same Institute for the construction of the electrical part of the probe.*

#### LIST OF SYMBOLS

$a$	wall oscillations amplitude	L
$c$	wave celerity	$LT^{-1}$
$E$	expected value	
$f$	wave frequency	$T^{-1}$
$f_s$	sampling frequency	$T^{-1}$
$g$	gravitational acceleration	$LT^{-2}$

$G$	estimation of power spectral density	$L^2T$
$h_0$	mean film thickness on motionless wall	$L$
$K$	coefficient of consistency	$ML^{-1}T^{n-2}$
$n$	flow behaviour index	
$N$	number of sampled data	
$P$	relative frequency	%
$Q$	flow rate	$L^2T^{-1}$
$Re$	Reynolds number (Eq. (2))	
$\Delta S$	relative surface enhancement	%
$t$	time	$T$
$t'$	temperature	$^{\circ}C$
$v$	velocity	$LT^{-1}$
$x, y$	Cartesian coordinates	$L$
$z$	dimensionless wave celerity	
$s^2$	estimation of variance	$L^2$
$\alpha$	dimensionless amplitude of sine wave	
$\dot{\gamma}$	shear rate	$T^{-1}$
$\delta$	local film thickness	$L$
$\delta_0$	mean film thickness	$L$
$\lambda$	wave length	$L$
$\omega$	angular frequency of wall oscillations	$T^{-1}$
$\rho$	density	$ML^{-3}$
$\sigma$	surface tension	$MT^{-2}$
$\mu$	viscosity	$MT^{-1}L^{-1}$
$\nu$	kinematic viscosity	$L^2T^{-1}$
$\tau$	shear stress	$MT^{-2}L^{-1}$
$\varphi$	function describing shape of film surface	

## REFERENCES

1. Perry F. H.: *Chem. Engr. Handbook*, p. 11. McGraw-Hill, New York 1963.
2. Sobolík V., Wein O., Mitschka P.: *Rheol Acta* 16, 394 (1977).
3. Dukler E.: *Progr. Heat Mass Transfer* 6, 207 (1972).
4. Hewitt G. F.: *Progr. Heat Mass Transfer* 6, 295 (1972).
5. Sylvester N. D., Tyler J. S., Skelland A. H. P.: *Can. J. Chem. Eng.* 51, 418 (1973).
6. Trojan Z.: *Thesis*. Technical University, Prague 1973.
7. Skelland A. H. P., Popadic V. O.: *Chem. Eng. Sci.* 8, 235 (1974).
8. Tekic M. N., Mitrovic M.: *Can. J. Chem. Eng.* 56, 460 (1978).
9. Sobolík V.: *Thesis*. Czechoslovak Academy of Sciences, Prague 1976.
10. Kapitza P. L.: *Zh. Exp. Teor. Fiz.* 18, 3 (1948).
11. Bendat J. S., Piersol A. G.: *Random Data: Analysis and Measurement Procedures*, Chapt. 9.6. Wiley, New York 1971.
12. Tailby S. R., Portalski S.: *Trans. Inst. Chem. Eng.* 38, 324 (1960).
13. Rejsek J.: *Thesis*. Czechoslovak Academy of Sciences, Prague 1980.

Translated by M. Rylek.